

LOCALISED CAPON SPECTRAL ESTIMATOR WITH APPLICATION TO THE PROCESSING OF NMR SIGNAL

Shanglin Ye and Elias Aboutanios

School of Electrical Engineering and Telecommunications,
University of New South Wales, Sydney, NSW 2052, Australia.

ABSTRACT

In this paper, we present a localised Capon spectral estimator that exhibits improved ability of resolving closely spaced peaks in the frequency domain. Starting with a unitary transformation using the discrete Fourier transform results in signals of interest being localised to small regions of the spectrum. Therefore, the algorithm uses this fact to construct a covariance matrix with low dimensionality, which can be easily inverted. This reduces the number of samples required to be averaged to produce the covariance matrix and as a result allows the spectrum resolution to be improved. In the simulation results, by comparing with the original Capon, the effectiveness of the novel estimator in resolving close peaks is demonstrated using both simulated undamped exponentials and simulated NMR spectroscopy signal (that is damped exponentials).

Index Terms— Capon spectral estimator, spectral estimation, spectrum resolution, NMR Spectroscopy.

1. INTRODUCTION

Spectral estimation is a fundamental research problem that is relevant to a wide range of engineering applications such as radar imaging, biomedical signal processing and speech processing (see [1] and the reference within). For instance, the signal in nuclear magnetic resonance (NMR) spectroscopy [2] [3] is modelled as a sum of an unknown number of decaying complex exponentials in additive noise [4]. The spectrum of the NMR data contains many closely spaced components that must be resolved. This necessitates a practical high resolution spectral estimator to detect and separate overlapping peaks.

When dealing with spectral estimation on signals with unknown number of components, such as NMR signals, popular high resolution parametric estimators [5] [6] are not desirable as they require the component number as a priori information. In the other hand, the Capon spectral estimator [7] and the amplitude and phase estimator (APES) [8], along with their efficient implementations [1] [9] are worth-considering methods as they are non-parametric spectral estimators that do not need the a priori information of the number of signal components. Their general philosophy relies on the design of adaptive FIR

filter-banks with each filter tuned to one of the frequency bins by solving certain constrained minimisations. The solution, however, involves the inversion of the covariance matrix of the signal. This covariance matrix must be estimated, which places hard requirements on the number of samples, and the inversion causes financial difficulties. Therefore, the achievable resolution of the estimated spectrum is limited by these two problems [8].

In this paper, we present a spectral estimator that has higher resolution than Capon and APES. To achieve this goal, we propose a localised version of the Capon estimator that reduces the dimensionality of the covariance matrix. This not only relieves the training data requirement, but also allows for a potentially lower computational complexity which can be traded for improved resolution.

The structure of the paper is as follows. In the following section, we review the original Capon spectral estimator. In Section 3, we put forward the novel localised Capon estimator. In Section 4, we show the simulation results of the localised algorithm, including the comparison with the original version on undamped exponentials and the application to simulated NMR signal. Finally the conclusions are drawn in Section 5.

2. CAPON SPECTRAL ESTIMATOR

Consider a signal modelled by:

$$x(n) = \sum_{i=1}^I a(f_i) e^{j2\pi f_i n} + w(n), \quad n = 0 \dots N-1 \quad (1)$$

where I is the number of components (usually unknown in practice). $a(f_i)$ is the complex spectrum amplitude corresponding to frequency f_i , which Capon estimator tempts to estimate. $w(n)$ is assumed to be additive Gaussian noise with zero mean and variance σ^2 .

In the original Capon spectral estimator, the signal samples are firstly partitioned to a $M \times L$ Hankel matrix $\mathbf{X} = [\mathbf{x}_1, \mathbf{x}_2, \dots, \mathbf{x}_L]$, where $\mathbf{x}_l = [x(l), x(l+1), \dots, x(l+M-1)]^T$ and $L = N - M + 1$ (note that $M < L$). Here $(\bullet)^T$ denotes the matrix transpose. The output signal filtered by an M -tap FIR filter $\mathbf{h}(f) \in C^{M \times 1}$ at time l is therefore given by

$y(l) = \mathbf{h}^H(f)\mathbf{x}_l$, where $(\bullet)^H$ denotes the conjugate transpose. The goal of the Capon estimator (filter) design is to minimise the power of the output signal \mathbf{y} , for a frequency of interest f , subject to the output of a single exponential signal at that frequency being constrained to 1. This is expressed as:

$$\min_{\mathbf{h}} \sum_{l=1}^L |\mathbf{h}^H(f)\mathbf{x}_l|^2 \quad \text{s.t.} \quad \mathbf{h}^H(f)\mathbf{s}_M(f) = 1 \quad (2)$$

where $\mathbf{s}_M(f) \in C^{M \times 1}$ is the Fourier template vector (single exponential signal) of length M :

$$\mathbf{s}_M(f) = [1, e^{j2\pi f}, \dots, e^{j2\pi(M-1)f}]^T. \quad (3)$$

The solution of this problem results in a filter-bank whose weights corresponding to f are:

$$\mathbf{h}(f) = \frac{\mathbf{R}^{-1}\mathbf{s}_M(f)}{\mathbf{s}_M^H(f)\mathbf{R}^{-1}\mathbf{s}_M(f)} \quad (4)$$

where \mathbf{R} is the signal covariance matrix. We use the forward-backward averaged covariance matrix throughout the paper:

$$\mathbf{R} = \frac{1}{2L} (\mathbf{X}\mathbf{X}^H + \tilde{\mathbf{X}}\tilde{\mathbf{X}}^H) \quad (5)$$

where $\tilde{\mathbf{X}}$ is the partition matrix of the complex conjugate reversed signal $\tilde{x}(n) = x^*(N-1-n)$ and $(\bullet)^*$ denotes the complex conjugate. We would like to mention here one may consider to use the forward-only covariance matrix to achieve higher resolution of the estimator (see [10]), however, we find that this is only true when M is relatively small. As M approaches L , the resolution of the forward-backward Capon becomes higher than the forward-only Capon. The amplitude spectrum estimation at frequency f is therefore $|\hat{a}(f)|$, where

$$\hat{a}(f) = \frac{1}{L} \mathbf{h}^H(f)\mathbf{X}\mathbf{s}_L^*(f) = \frac{\mathbf{s}_M^H(f)\mathbf{R}^{-1}\mathbf{X}\mathbf{s}_L^*(f)}{L\mathbf{s}_M^H(f)\mathbf{R}^{-1}\mathbf{s}_M(f)}. \quad (6)$$

3. LOCALISED CAPON SPECTRAL ESTIMATOR

It is known that choosing a larger filter length M will result in higher resolution of the spectrum estimation in (6) whereas the amount of averaging, L , controls the smoothness. In order to obtain a non-singular (invertible) covariance matrix \mathbf{R} , the number of samples being averaged must be strictly larger than the number of degrees of freedom, that is $M < L$. Therefore, for any fixed N , the Capon algorithm appears to have a limit on the achievable resolution of the spectrum estimation. We now present the localised Capon estimator that allows us to relax the averaging requirement and improve the resolution.

Let $\mathbf{F} \in C^{M \times M}$ be the unitary Fourier matrix having $\frac{1}{\sqrt{M}}\mathbf{s}_M(f)$ as one of its columns, Eq. (6) can be re-written as

$$\begin{aligned} \hat{a}(f) &= \frac{\mathbf{s}_M^H(f)\mathbf{F}\mathbf{F}^H\mathbf{R}^{-1}\mathbf{F}\mathbf{F}^H\mathbf{X}\mathbf{s}_L^*(f)}{L\mathbf{s}_M^H(f)\mathbf{F}\mathbf{F}^H\mathbf{R}^{-1}\mathbf{F}\mathbf{F}^H\mathbf{s}_M(f)} \\ &= \frac{[\mathbf{F}^H\mathbf{s}_M(f)]^H(\mathbf{F}^H\mathbf{R}\mathbf{F})^{-1}[\mathbf{F}^H\mathbf{X}\mathbf{s}_L^*(f)]}{L[\mathbf{F}^H\mathbf{s}_M(f)]^H(\mathbf{F}^H\mathbf{R}\mathbf{F})^{-1}[\mathbf{F}^H\mathbf{s}_M(f)]}. \end{aligned} \quad (7)$$

Now it is clear that $\mathbf{F}^H\mathbf{s}_M(f) = [0, \dots, 0, 1, 0, \dots, 0]^T$ with all of the energy of $\mathbf{s}_M(f)$ concentrated in the element corresponding to the column index of $\frac{1}{\sqrt{M}}\mathbf{s}_M(f)$. Therefore, we propose reducing the dimensionality of the problem to $r \ll M$ by localising the Fourier matrix \mathbf{F} to a matrix $\bar{\mathbf{F}}$ consisting of only a few column vectors around $\mathbf{s}_M(f)$. In the following, the overbar refers to the dimension reduced quantities. Then $\bar{\mathbf{F}}^H\mathbf{s}_M(f)$ becomes a length- r vector that has 1 for the entry corresponding to f and zero elsewhere. Let $r = 2p + 1$, then the reduced dimension vector $\bar{\mathbf{s}}_r$ becomes

$$\bar{\mathbf{s}}_r(f) = \bar{\mathbf{F}}^H\mathbf{s}_M(f) = \underbrace{[0, \dots, 0]}_p, \underbrace{[1, 0, \dots, 0]}_p]^T. \quad (8)$$

Clearly the localised algorithm reverts to the original if we put $r = M$.

When the DFT is oversampled by zero-padding the signal $x(n)$ prior to the FFT algorithm, \mathbf{F} becomes not a unitary matrix and (8) no longer holds. Nevertheless, we can still make the assumption that most of the energy of $\mathbf{F}^H\mathbf{s}_M(f)$ is concentrated in a small number of points in the neighbourhood of the frequency of interest f . Let the zero padding be to a length $N_F = mM$ for $m > 0$. Then for $\mathbf{F} \in C^{N_F \times N_F}$ we can still perform the localisation $\bar{\mathbf{s}}_r(f) = \bar{\mathbf{F}}^H\mathbf{s}_M(f)$ with $\bar{\mathbf{F}}$ having the center column on f and another $2p$ columns spaced by $\lfloor m \rfloor$ bins, where $\lfloor \bullet \rfloor$ is the floor operation.

Now the localised Fourier-transformed signal matrix is $\tilde{\mathbf{X}} = \bar{\mathbf{F}}^H\mathbf{X}$ (similarly $\tilde{\mathbf{X}} = \bar{\mathbf{F}}^H\tilde{\mathbf{X}}$ for reversed signal matrix) and the localised Fourier-transformed covariance matrix becomes

$$\bar{\mathbf{R}} = \bar{\mathbf{F}}^H\mathbf{R}\bar{\mathbf{F}} = \frac{1}{2L} (\tilde{\mathbf{X}}\tilde{\mathbf{X}}^H + \tilde{\mathbf{X}}\tilde{\mathbf{X}}^H). \quad (9)$$

The localised Capon spectral estimator is then given by:

$$\tilde{a}(f) = \frac{\bar{\mathbf{s}}_r^H(f)\bar{\mathbf{R}}^{-1}\tilde{\mathbf{X}}\mathbf{s}_L^*(f)}{L\bar{\mathbf{s}}_r^H(f)\bar{\mathbf{R}}^{-1}\bar{\mathbf{s}}_r(f)}. \quad (10)$$

To calculate (10) for each frequency bin, operations on small size matrices related to r are performed, which significantly reduces the dimensionality of the original algorithm. Also, instead of the original $M \times M$ covariance matrix, we now require $L_r > r$ vectors to be averaged for the localised covariance matrix $\bar{\mathbf{R}} \in C^{r \times r}$ to be invertible. This relaxation of the required amount of smoothing allows us to reduce L below the initial limit of M . The consequence of this is that M can be increased (recall that $L + M - 1 = N$), which leads to an improved spectral resolution with respect to the original algorithm. For a good balance between smoothness of the spectrum and resolution, we found that a smoothing length satisfying $\frac{N}{4} < L_r \leq \frac{N}{2}$ works well.

Finally, we summarise the localised Capon spectrum estimation algorithm as:

1. Given a signal vector $\mathbf{x} \in C^{1 \times N}$, use partitioning strategy to generate $M \times L_r$ Hankel signal matrices \mathbf{X} and $\tilde{\mathbf{X}}$, where $\frac{N}{4} < L_r \leq \frac{N}{2}$ and $M = N - L_r + 1$;

2. Initialise the localised region r (typically $r = 5, 7, 9$), the frequency grid $\mathbf{f} \in C^{1 \times N_F}$ and the Fourier templates $\mathbf{s}_M(\mathbf{f}) \in C^{M \times N_F}$;
3. According to the frequency grid \mathbf{f} , calculate $\mathbf{F}^H \mathbf{X}$, $\mathbf{F}^H \tilde{\mathbf{X}}$ and $\mathbf{F}^H \mathbf{s}_M(\mathbf{f})$ using N_F -FFT;
4. For each bin f in the frequency grid, do:
 - (a) Center a sliding window of length r , which has all of its points spaced by $\lfloor \frac{N_F}{M} \rfloor$ bins, on the corresponding column of f in $\mathbf{F}^H \mathbf{X}$ and $\mathbf{F}^H \tilde{\mathbf{X}}$ to obtain $\tilde{\mathbf{X}} \in C^{r \times L}$ and $\tilde{\tilde{\mathbf{X}}} \in C^{r \times L}$;
 - (b) Use the same sliding window and obtain $\tilde{\mathbf{s}}_r(f) \in C^{r \times 1}$ from $\mathbf{F}^H \mathbf{s}_M(\mathbf{f})$
 - (c) Calculate $\tilde{\mathbf{R}} \in C^{r \times r}$ using (9) and find $\tilde{\mathbf{R}}^{-1}$;
 - (d) Obtain the spectrum estimation $\tilde{a}(f)$ using (10).

Although a full analysis of the computational cost of the localised algorithm is beyond the scope of this paper, it is worth including some comments on it before concluding this section. The localised algorithm requires the inversion of a much smaller matrix than the original Capon ($r \ll M$). This significantly reduces the computational cost per frequency bin and it remains much smaller than the original Capon for a reasonable number of bins. However, in the case that the spectrum is required to be calculated on the whole spectrum with a dense grid, direct implementation of the localised version can become burdensome with respect to efficient implementations of the original Capon [1, 9]. Note, however, that analysing the entire spectral bandwidth is not necessary in NMR spectroscopy as the signals of interest usually occupy several small frequency regions. Nevertheless, efficient implementations of the localised version are being investigated.

4. SIMULATION RESULTS

In this section, we first simulate the proposed localised Capon spectral estimator on simulated undamped signal and compare the performance with the original Capon and other well known estimation algorithms including APES and the MUSIC estimator [6] (which needs the number of components in advance). Then we apply the proposed estimator to a simulated NMR signal to further demonstrate the performance.

We first compare the ability of the various estimators to resolve two closely spaced peaks by performing the algorithms on a sum of two undamped complex exponentials:

$$x(n) = e^{j2\pi f_1 n} + e^{j\theta} e^{j2\pi f_2 n} + w(n), \quad n = 0 \dots N-1 \quad (11)$$

where $N = 64$. θ is the phase difference between the two components and $f_1, f_2 \in [0, 1]$ are normalised frequencies. The noise terms $w(n)$ are zero-mean Gaussian noise with variance σ^2 . The signal to noise ratio (SNR) is defined by $1/\sigma^2$. In this simulation, we set $\theta = 0$, SNR = 25dB, $f_1 = 0.5$ and

vary f_2 from 0.495 to 0.499. We consider two closely spaced sinusoidal signals as resolved if the following rule is satisfied [10]:

$$\delta = 2\hat{a}(f_m) - \hat{a}(f_1) - \hat{a}(f_2) < 0 \quad (12)$$

where $\hat{a}(f)$ is the spectrum estimation at frequency f and $f_m = 0.5(f_1 + f_2)$, which is the intermediate frequency between f_1 and f_2 . For the localised Capon, we use a localised region $r = 5$. For the original Capon, we consider to obtain the highest achievable resolution by putting $M = 0.5N = 32$, giving $L = M + 1 = 33$. For both MUSIC and APES, we use the same covariance matrix as the original Capon. Fig. 1 shows the rate of successfully resolving both peaks as a function of f_2 . We find that when $L_r = 20$, the localised algorithm has a much stronger ability to separate two peaks than original Capon and APES, and is also slightly better than the MUSIC estimator. As $L_r \rightarrow L$, the performance of the localised algorithm is comparable to Capon and APES.

Then we examine the accuracy of frequency estimation of different methods. In this simulation, we use the previous signal model (11) by setting $f_1 = 0.5$ and $f_2 = 0.48$. θ is randomly chosen in each run. We obtain the frequency estimates of the Capon algorithms by peak picking in the estimated amplitude spectra. As it has already been shown in [10] that the Capon estimator significantly outperforms APES for frequency estimation, the result of APES is not shown in this simulation. The parameters of localised Capon, Capon and MUSIC are the same as the previous test. Fig. 2 shows the root mean square error (RMSE) of the estimates of f_1 versus SNR. For comparison, we also show the Cramer-Rao lower bound (CRLB) of multiple exponentials case. It can be clearly found that for all the estimators, the RMSEs follow the trend of the CRLB. The MUSIC estimator has similar performance to the original Capon. We know that smaller L_r leads to a less smoothed spectrum estimation. Therefore, the RMSE of localised Capon when $L_r = 20$ is marginally larger, and it becomes more comparable to the other two estimator as L_r approaches L . This also illustrates the trade-off that exists between the resolution and the RMSE.

Next, we examine the ability for resolving three closely spaced peaks by applying all the algorithms to the signal:

$$x(n) = \sum_{i=1}^3 e^{j2\pi f_i n} + w(n), \quad n = 0 \dots 63 \quad (13)$$

where $f_1 = 0.5$ and $f_2 = 0.495$, which are previously shown to be resolvable in the two components case for all the estimators. We set SNR = 25dB and f_3 varies from 0.45 to 0.49. As f_3 becomes closer to f_2 , we say all the three components are successfully resolved if f_1 and f_2 are resolved and at the same time f_3 and f_2 are also resolved. The parameters of all the algorithms are set to the same values as the previous tests. Fig. 3 shows the rate of resolving all the components as a function of the varying f_3 . We find the figure exhibit similar

results as the two components case that localised Capon when $L_r = 20$ is the most capable estimator to resolve all the peaks.

To conclude the above three simulations, the localised Capon outperforms the original version in both resolution and accuracy of frequency estimation, and at the same time outperforms the original Capon for resolution by sacrificing slight loss on accuracy. In small L_r case, the localised Capon has higher resolution than MUSIC but has higher RMSE as well. Nevertheless, we would like to emphasize that the advantages of the localised Capon are still obvious: MUSIC requires the signal components as a priori knowledge, which is not needed in localised Capon; Also, as the number of signal samples becomes large (i.e. $N \geq 2^{10}$, which is the common case in NMR signal), MUSIC becomes undesirable due to the heavy computational cost of the eigenvalue decomposition of a huge covariance matrix, while the localised Capon is still implementable as localised covariance matrices are to be inverted. And clearly, these advantages can also be applied to other parametric estimators such as ESPRIT [5].

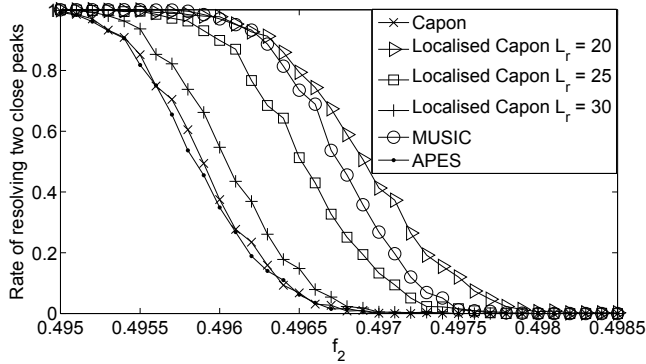


Fig. 1. Ability of resolving two closely spaced peaks of various algorithms. 1,000 Monte Carlo runs were used.

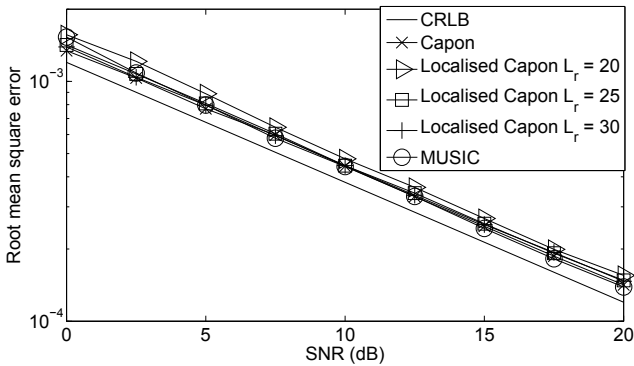


Fig. 2. RMSE of frequency estimation obtained by various algorithms. 5,000 Monte Carlo runs were used.

Finally, we demonstrate the performance of the Capon and localised Capon estimators to the processing of simulated

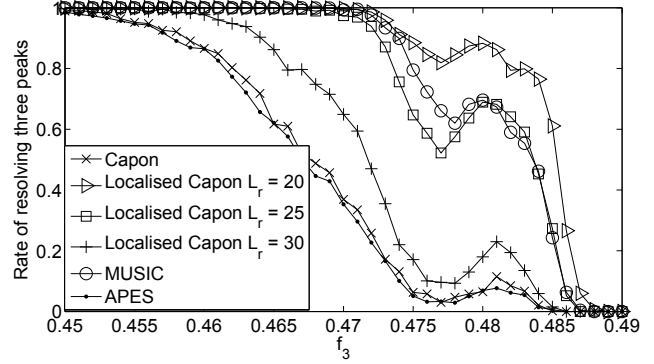


Fig. 3. Ability of resolving three closely spaced peaks of various algorithms. 1,000 Monte Carlo runs were used.

Table 1. Parameters of the simulated NMR signal

Component Number	Amplitude	Frequency	Damping Factor
1	5	0.2	5×10^{-3}
2	0.1	0.498	1×10^{-4}
3	1	0.5	5×10^{-4}
4	1	0.5005	5×10^{-4}
5	0.1	0.5025	1×10^{-4}
6	0.2	0.698	2.5×10^{-3}
7	0.5	0.7	1×10^{-4}

NMR signal. The signal consists of a sum of seven damped complex exponentials:

$$x(n) = \sum_{i=1}^7 e^{j\phi} A_i e^{(-\eta_i + j2\pi f_i)n} + w(n), \quad n = 0 \dots N-1 \quad (14)$$

where $N = 1024$. A_i , $\eta_i > 0$ and f_i are the complex amplitude, the damping factor and the frequency of the i^{th} component respectively. ϕ denotes the initial phase, which we set to be zero. The noise variance is set to $\sigma^2 = 0.01$ and the signal parameters are listed in Table 1. The signal components are chosen so that components 3 and 4 are very close to each other, with two satellites located either side of them. Component 6 and 7 are closely spaced as well with one of them being more damped than another. In this simulation, we mainly focus the ability of resolving peaks on the spectrum.

To show the superiority of peak resolving of the Capon algorithms, we “zoom in” the spectrum by showing the Capon and localised Capon spectrum estimation on the frequency bins around $f = 0.5$ and $f = 0.7$. The smoothing length of the original Capon used here is $L = N/2 + 1 = 513$ and that of the localised Capon is $L_r = \lfloor \frac{N}{3} \rfloor = 341$. The size of the localised region is set to $r = 9$. For both algorithms, the frequency bins calculated are spaced by $1/N_F$, where $N_F = 2^{17}$. For comparison, we also plot the absolute value of the real part of N_F -point DFT (as it has stronger peak-resolving ability than the absolute-valued DFT). In Figs. 4 and 5 we demon-

strate the “zoomed in” spectra by plotting all the algorithms on top of each other and normalising the amplitude. It can be clearly found in Fig. 4 that the closely spaced peaks which are not separated in the DFT can now be clearly observed using Capon estimators where the energy of the components are more concentrated near the true frequencies. Furthermore, note how the localised Capon shows a much improved resolution, especially for the two large peaks. In Fig. 5 we see that the Capon estimators reduce the sidelobes due to the large component and show component 6 more clearly than the DFT.

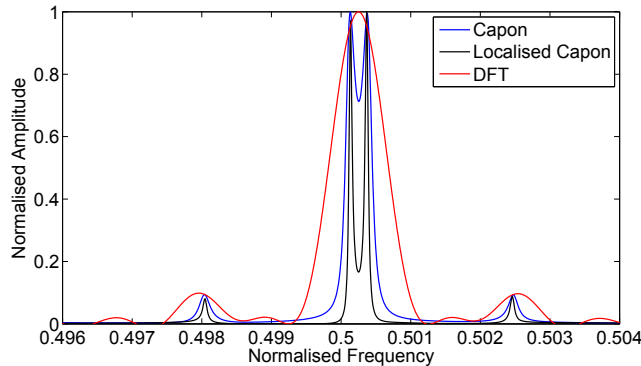


Fig. 4. The performance of the estimators near $f = 0.5$ of the simulated NMR spectrum.

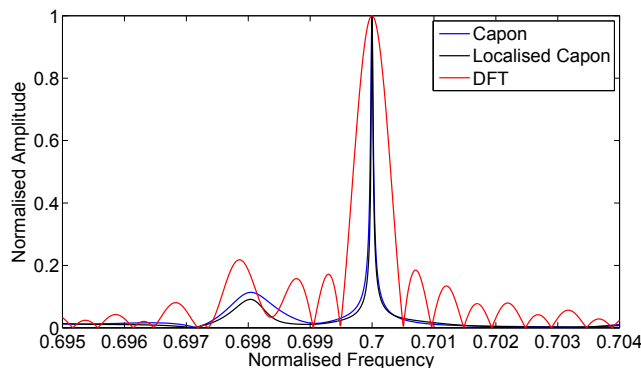


Fig. 5. The performance of the estimators near $f = 0.7$ of the simulated NMR spectrum.

5. CONCLUSIONS

We have presented in this paper a localised version of the Capon spectral estimator for resolving closely spaced peaks in the frequency domain. Instead of finding the inverse of the whole signal covariance matrix, the novel method localises the covariance matrix into a small area of the spectrum centered on the signal of interest. Consequently, a larger amount of the available data can be used to improve the spectrum res-

olution. Simulation results show the localised algorithm have stronger capability to resolve close peaks but slightly higher variance than original Capon estimator and its superiority on component detection is further confirmed by experimenting on simulated NMR signal.

6. REFERENCES

- [1] G.-O. Glentis, “A fast algorithm for APES and Capon spectral estimation,” *IEEE Transactions on Signal Processing*, vol. 56, no. 9, pp. 4207–4220, 2008.
- [2] R.S. Macomber, *A complete introduction to modern NMR spectroscopy*, Wiley-Interscience publication, Wiley, 1998.
- [3] J.K. Nicholson, J. Connelly, J.C. Lindon, and E. Holmes, “Metabonomics: A platform for studying drug toxicity and gene function,” *Nature Reviews Drug Discovery*, vol. 1, no. 2, pp. 153–161, 2002.
- [4] S. Umesh and D.W. Tufts, “Estimation of parameters of exponentially damped sinusoids using fast maximum likelihood estimation with application to NMR spectroscopy data,” *IEEE Transactions on Signal Processing*, vol. 44, no. 9, pp. 2245–2259, 1996.
- [5] R. Roy and T. Kailath, “ESPRIT - estimation of signal parameters via rotational invariance techniques,” *IEEE Transactions on Acoustics, Speech, and Signal Processing*, vol. 37, no. 7, pp. 984–995, 1989.
- [6] R. O. Schmidt, “Multiple emitter location and signal parameter estimation,” *IEEE Transactions on Antennas and Propagation*, vol. AP-34, no. 3, pp. 276–280, 1986.
- [7] J. Capon, “High-resolution frequency-wavenumber spectrum analysis,” *Proceedings of the IEEE*, vol. 57, no. 8, pp. 1408 – 1418, 1969.
- [8] J. Li and P. Stoica, “An adaptive filtering approach to spectral estimation and SAR imaging,” *IEEE Transactions on Signal Processing*, vol. 44, no. 6, pp. 1469–1484, 1996.
- [9] E.G. Larsson and P. Stoica, “Fast implementation of two-dimensional APES and Capon spectral estimators,” *Multidimensional Systems and Signal Processing*, vol. 13, no. 1, pp. 35–53, 2002.
- [10] A. Jakobsson and P. Stoica, “Combining Capon and APES for estimation of spectral lines,” *Circuits, Systems, and Signal Processing*, vol. 19, no. 2, pp. 159–169, 2000.